Induction of Lrp5 HBM-causing mutations in Cathepsin-K expressing cells alters bone metabolism.

Authors: Kyung Shin Kang[1,2,3], Jung Min Hong[4], Daniel J. Horan[1], Kyung-Eun Lim[1], Whitney A. Bullock[1], Angela Bruzzaniti[4], Steven Hann[5], Matthew L. Warman[5,6], and Alexander G. Robling[1,2,4]*

Affiliations:

[1]Department of Anatomy & Cell Biology, Indiana University School of Medicine, Indianapolis, IN, USA

[2]Richard L. Roudebush VA Medical Center, Indianapolis, IN, USA

[3]School of Physical Science & Engineering, Anderson University, Anderson, IN, USA

[4]Department of Biomedical & Applied Sciences, Indiana University School of Dentistry, Indianapolis, IN, USA

[5]Department of Orthopaedic Surgery, Boston Children's Hospital, Boston, MA, USA

[6]Howard Hughes Medical Institute, Department of Genetics, Harvard Medical School, Boston, MA, USA

[7]Department of Biomedical Engineering, Indiana University–Purdue University at Indianapolis, Indianapolis, IN, USA

Running Head: Lrp5 mutations in osteoclasts

Keywords: Lrp5, HBM, osteoclasts, resorption, Ctsk

Disclosure Statement: The authors have nothing to disclose.

***Corresponding Author**:

Alexander G. Robling, Ph.D.
Department of Anatomy & Cell Biology
Indiana University School of Medicine
635 Barnhill Dr., MS 5035
Indianapolis, IN 46202
Tel: (317) 274-7489
Fax: (317) 278-2040
Email: arobling@iupui.edu

Grant support:

This work was supported by NIH grants AR053237 (to AGR and MLW) and VA grant BX001478 (to AGR).

ABSTRACT

High-bone-mass (HBM)-causing missense mutations in the low density lipoprotein receptor-related protein-5 (Lrp5) are associated with increased osteoanabolic action and protection from disuse- and ovariectomy-induced osteopenia. These mutations (e.g., A214V and G171V) confer resistance to endogenous secreted Lrp5/6 inhibitors, such as sclerostin (SOST) and Dickkopf homolog-1 (DKK1). Cells in the osteoblast lineage are responsive to canonical Wnt stimulation, but recent work has indicated that osteoclasts exhibit both indirect and direct responsiveness to canonical Wnt. Whether Lrp5-HBM receptors, expressed in osteoclasts, might alter osteoclast differentiation, activity, and consequent net bone balance in the skeleton, is not known. To address this, we bred mice harboring heterozygous Lrp5 HBM-causing conditional knock-in alleles to Ctsk-Cre transgenic mice and studied the phenotype using DXA, μCT, histomorphometry, serum assays, and primary cell culture. Mice with HBM alleles induced in Ctsk-expressing cells (TG) exhibited higher bone mass and architectural properties compared to non-transgenic (NTG) counterparts. *In vivo* and *in vitro* measurements of osteoclast activity, population density, and differentiation yielded significant reductions in osteoclast-related parameters in female but not male TG mice. Droplet digital PCR performed on osteocyte enriched cortical bone tubes from TG and NTG mice revealed that ~8-17% of the osteocyte population (depending on sex) underwent recombination of the conditional Lrp5 allele in the presence of Ctsk-Cre. Further, bone formation parameters in the midshaft femur cortex shows a small but significant increase in anabolic action on the endocortical but not periosteal surface. These findings suggest that Wnt/Lrp5 signaling in osteoclasts affects osteoclastogenesis and activity in female mice, but also that some of the changes in bone mass in TG mice might be due to Cre expression in the osteocyte population.

INTRODUCTION

Most FDA-approved therapies for osteoporosis target the bone-resorbing activities of osteoclasts(1). More recently, anabolic treatments have been considered a promising approach to improve bone properties. Approved agents that stimulate anabolic action are focused around the PTH/PTHrP axis, but discoveries regarding anabolic potential of the Wnt signaling pathway have provided other avenues to achieve anabolism in bone (2, 3). Several plasma membrane receptors are involved in the Wnt signaling pathway, including the low density lipoprotein receptor-related protein-5 (LRP5). Numerous reports indicate that LRP5 is a key protein involved in the regulation of bone mass (4). The importance of LRP5 in skeletal regulation has been addressed using genetically engineered mouse models, all of which consistently show significant changes in bone mass and strength with gain- and loss-of function mutations in the gene (5-9).

Much of the high bone mass (HBM) phenotype described in mice with LRP5 HBM-causing mutations (e.g. Lrp5-HBM transgene or knock-in point mutations) has been ascribed to altered anabolic signaling in the osteoblast/osteocyte. Mice with HBM-causing missense mutations in *Lrp5* provide robust gain-of-function models because LRP5 HBM receptors respond normally to Wnt ligands but exhibit resistance to endogenous inhibitors such as sclerostin (SOST) and Dickkopf homolog-1 (DKK1) (10-13). Additionally, these mutations enhance responsiveness to mechanical loading and protect the skeleton from the bone-wasting effects of mechanical disuse (14, 15).

While most of the published reports on Wnt action in bone have focused on the anabolic effects in osteoblasts, or on the anabolism-relaying effects in osteocytes, much less is known about Wnt signaling in osteoclasts. Osteoclasts are modulated by Wnt proteins, secreted by neighboring osteoblasts and osteocytes (16). Beyond indirect effects on the osteoclast (e.g., Wnt-modulated RANKL/OPG production by osteocytes/osteoblasts), more recent data suggest that Wnt stimulation can have direct effects on osteoclasts (17). The most thoroughly characterized mechanism for direct osteoclast stimulation by Wnt is the Wnt5a/Ror2 pathway, which activates one of the non-canonical arms of intracellular Wnt signaling (18). However, osteoclasts also express the molecular machinery to transduce canonical Wnt signaling (e.g., LRP5/6, FZDs, β-catenin, GSK3β) (19), and deletion of LRP5/6 in early osteoclasts results in increased resorption and low bone mass, whereas treatment of osteoclast cultures with the canonical ligand Wnt3a induces β-catenin nuclear translocation and suppresses osteoclast differentiation (17). In light of the accumulating evidence that canonical Wnt signaling might have a significant role in the osteoclast, we hypothesized that osteoclast-selective (i.e., *Ctsk*-Cre-mediated) expression of LRP5 receptors harboring the HBM-causing G171V or A214V mutations would exhibit increased bone mass via Wnt-mediated inhibition of osteoclasts.

In this communication, we sought to investigate whether expression of LRP5 gain-of-function mutations (G171V, A214V) in osteoclasts would alter bone homeostasis *in vivo* and osteoclastogenesis *in vitro*. Mice harboring heterozygous *Lrp5* HBM-causing conditional knock-in alleles were bred with Ctsk-Cre transgenic mice. We evaluated *in vivo* actions of both *Lrp5* mutant alleles individually, expressed in osteoclasts, on bone mass and degradation. We also explored the *in vitro* effects of the mutations on osteoclast differentiation and activity, using bone marrow hematopoietic stem cells

isolated from the mutant mice. Here, we report that *Lrp5* HBM-causing knock-in alleles in *Ctsk*-expressing cells significantly increase overall bone mass and reduce resorption in female mice, but have more mild effects in male mice.

MATERIALS AND METHODS

Experimental Mice

Mice with *Lrp5* conditional knockin alleles for HBM-causing mutations A214V and G171V have been described previously (5). These alleles, *Lrp5*^{A_N} and *Lrp5*^{G_N}, respectively) are activated by Cre-recombination. Male mice with conditional *Lrp5* alleles were crossed to hemizygous female *Ctsk*-Cre transgenic (TG) mice, which is expressed in osteoclasts (20). Offspring with the following genotypes were studied TG;+/A (mice with the Lrp5^{A_N} allele and the *Ctsk*-Cre transgene), NTG;+/A (mice with the Lrp5^{A_N} allele but not the *Ctsk*-Cre transgene), TG;+/G (mice with Lrp5^{G_N} allele and the *Ctsk*-Cre transgene), and NTG;+/G (mice with the Lrp5^{G_N} allele but not the *Ctsk*-Cre transgene). The genetic background of all mice was a mixture of 129S1/SvIMJ and C57Bl/6J. Offspring were same sex–housed in cages of 3 to 5 (independent of *Ctsk*-Cre genotype) and given standard mouse chow [Harlan Teklad 2018SX; 1% Ca; 0.65% P; vitamin D3 (2.1 IU/g)] and water ad libitum. The *Lrp5* alleles and the *Ctsk* –Cre transgene were genotyped using standard PCR on genomic DNA from ear notches. All animal procedures were performed in accordance with relevant federal guidelines and conformed to the Guide for the Care and Use of Laboratory Animals (8th Edition). The animal facility at Indiana University is an AAALAC-accredited facility.

Dual-energy x-ray absorptiometry (DEXA)

Whole-body DEXA scans were collected on isoflurane-anesthetized mice using a PIXImus II (GE Lunar, Madison, WI) densitometer. All experimental mice were scanned at 7, 10, and 15 weeks of age as indicated in Fig 1A. From the whole body scans, areal bone mineral density (BMD) and bone mineral content (BMC) were calculated for the entire postcranial skeleton using the Lunar ROI tools.

Micro-computed tomography (μCT)

The right femur was extracted at sacrifice (16 weeks of age) and fixed in 4% PBF for 2 days, then transferred into 70% ethanol. A 2.6-mm span of the distal femoral metaphysis was scanned on a desktop μCT (μCT 20; Scanco Medical AG) at 13-μm resolution using 70-kV peak tube potential and 151-ms integration time to measure trabecular three-dimensional morphometric properties as previously described (21). Standard trabecular bone parameters (BV/TV, Tb.N, Tb.Th) were calculated from each reconstructed stack through the metaphysis. Cortical thickness (Ct. Th) and area (Ct.Ar) were obtained from 20 slices reconstructed through the midshaft femur at 9-μm resolution.

Measurements of serum bone resorption markers and osteoclast enumeration in mice

To measure levels of the serum resorption marker carboxy-terminal collagen cross-links (CTx), blood samples were collected from each mouse at 7 weeks of age, allowed to clot for 30 to 60 minutes, and then centrifuged to separate and collect serum. CTx was measured from the serum using a commercially available plate assay (IDS Ratlaps EIA, Gaithersburg, MD) following the manufacturer's instructions. Serum samples from 10 mice per group were analyzed. Additionally, after conducting μCT measurements on the right femur, we processed those tissues for plastic-embedded thin sectioning and Trap-staining as described previously (22). Osteoclast number per unit bone surface (Oc.N/BS, #/mm) and osteoclast surface per unit bone surface (Oc.S/BS, %) were measured in metaphyseal cancellous bone.

Osteoclast culture and osteoclastogenic assays

Bone marrow-derived macrophages (BMMs) were prepared as previously described (23). Briefly, bone marrow was isolated from 6-week old mice heterozygous for the *Lrp5* G171V conditional allele (G171V), with or without the *Ctsk*-Cre transgene. After culturing for 24 h in α-MEM containing 10% FBS, non-adherent cells were collected and cultured in α-MEM containing 10% FBS with M-CSF and RANKL (PeproTech, NJ, USA) For osteoclastogenesis assays, cells were plated at 6×10^4 cells/well in a 96 well plate and cultured for 4-5 days until the appearance of multinucleated osteoclasts. The osteoclasts were then fixed in 4% paraformaldehyde for 10 min and then stained for TRAP with 0.1 M acetate solution (pH 5.0) containing 6.7 mM sodium tartrate, 0.12 mg/ml naphthol AS-MX phosphate, and 0.07 mg/ml fast red violet. After TRAP staining, the numbers of red-stained TRAP-positive cells that had more than three nuclei and a red cytosol were counted under a light microscope. The average was calculated from 5 wells of 96-well plates. This counting was repeated five times. To determine the bone resorption activity of osteoclasts, multinucleated osteoclasts cultured in the presence of RANKL and M-CSF for 4-5 days were treated with 0.025% trypsin-EDTA for 3-5 min (with light mechanical scraping) to release the cells. The detached mature osteoclasts were washed in growth media, and an identical number of cells were reseeded onto sterilized cortical bone slices (approx. 200 osteoclasts per slice in 96 well plates; IDS, Ltd, Boldon, UK). After 3 days of culture on bone slices, the conditioned media was collected for biochemical evaluation of osteoclast resorption activity (CTx ELISA, IDS Inc., Gaithersburg, MD). The bone slices were TRAP stained for osteoclast enumeration, and the osteoclast counts were used to normalize the CTx data (CTx/OC number). To stain osteoclast resorption pits, the TRAP-stained cells on bone slices were first removed using mechanical agitation, and the slices were incubated with 20 μg/ml of peroxidase-conjugated wheat germ agglutinin for 45 min, followed by the staining of the pits with chromogen 3,3′-diaminobenzidine (Sigma-Aldrich, St Louis, MO). To quantify the resorption on each bone slice, the resorbed pits were identified and measured for area using ImageJ.

Gene expression of osteoclast-selective transcripts using quantitative PCR

Non-adherent bone marrow cells were prepared as described above and cultured with M-CSF alone to form macrophages (50 ng/ml M-CSF for 3 days) or with M-CSF plus RANKL to form pre-osteoclasts (20 ng/ml M-CSF plus 80 ng/ml RANKL for 3 days) and mature osteoclasts (20 ng/ml M-CSF plus 80 ng/ml RANKL for 5 days). The formation of pre-osteoclasts and mature osteoclasts was confirmed based on their morphology. RNA was isolated from the cell preparations using Qiagen RNeasy kits, and the cDNAs were synthesized from 1 μg of RNA using SuperScript synthesis system (Invitrogen). Quantitative RT-PCR was performed on an ABI 7900HT Real time PCR system (Applied Biosystems) using SYBR Green PCR Master Mix assay (Applied Biosystems) for the following transcripts: *Oscar*, *Dcstamp*, *Ctsk*, *Clcn7*, and *Atp6ap1*. Primer sequences are listed in Table S1. The amplification reaction was performed for 40 cycles with denaturation at 95°C for 10 minutes, followed by annealing at 95°C for 15 seconds and extension and detection at 60°C for 1 minute. Gene expression was quantitated using the $2^{-\Delta\Delta C_T}$ method and normalized to transcripts for the housekeeper GAPDH.

Droplet digital PCR assay for genomic recombination of the conditional Lrp5-HBM alleles

Droplet digital PCR (ddPCR) was performed as previously described (24). Briefly, epiphyseal ends of bone were removed from cleaned long bones and the bone marrow removed by extensive washing with PBS. DNA was extracted from bone pieces using the DNeasy Blood and Tissue Kit (Qiagen) and ~ 3 ng of cortical bone DNA was used in subsequent PCR reactions. Supermix for Probes mastermix (BioRad, Hercules, CA) was used following the manufacturer's recommendations. PCR was performed using Eppendorf EP gradient S machines, nanodroplets were created using an automatic droplet generator, amplimer containing droplets were counted with a QX200 sample reader, and data were analyzed using Quantasoft software (all instrumentation from BioRad). The primer pairs and probes described below were purchased from IDT (Coralville, IA) and were used to amplify and quantify the number conditional and recombined alleles. At least 200 amplimer-containing droplets per animal were created in order to measure Cre-mediated recombination. PCR primers, P26-AGTACTGGCTGGCACAGA, P27-CAGGCTGCCCTTGCAGAT, and P28-GTCAGTTTCATAGCCTGA were combined and used in a single PCR reaction to generate a 320-bp amplimer for the conditional allele and a 400-bp amplimer for the recombined allele. The conditional allele was detected using a 5HEX/CCGCAAGCTCTAGAGTCAGCTTCTGAT/3IABkFQ probe, while the recombined allele was detected using a 56-FAM/CGGAATTTAGAGGATCCCCGGGTACC/3IABkFQ probe. PCR parameters were run as follows: 95°C for 10 minutes; 94°C for 30 seconds, 57°C for 60 seconds, 72C for 30 seconds, for 40 cycles at 20% ramp; 98°C for 10 minutes, and then 12°C indefinitely.

Quantitative histomorphometry

Demeclocycline (60 mg/kg IP) and calcein (12 mg/kg IP) were injected at 7 and 15 weeks of age, respectively. After collecting left femurs at sacrifice (17 weeks of age), the 4% PBF-fixed femurs were dehydrated in graded ethanols, cleared in xylene, and embedded in methylmethacrylate (MMA). Thick sections were cut from the midshaft using a diamond-embedded wafering saw. Sections were ground and polished to ~30 μm, mounted and coverslipped, then digitally imaged on a fluorescent microscope. Periosteal and endocortical bone formation parameters were calculated by measuring the extent of unlabeled perimeter (nL.Pm), single-labeled perimeter (sL.Pm), double-labeled perimeter (dL.Pm), and the area between the double labeling with Image-Pro software (MediaCybernetics Inc., Gaithersburg, MD). The derived histomorphometric parameters mineralizing surface over bone surface (MS/BS), mineral apposition rate (MAR), and bone formation rate (BFR/BS) were calculated using standard procedures described elsewhere (25).

Statistical methods

Statistical analyses were computed using two-way ANOVA, with *Ctsk*-Cre genotype, TG(transgenic) or non-NTG (non-transgenic), and *Lrp5* genotype, +/A or +/G, as main effects. Significant main effects were followed up with all-pairwise post-hoc comparisons using Fishers protected LSD tests. Significance was taken at $p < 0.05$. All data are presented as mean ± SEM.

RESULTS

Increased bone mass in mice with activated Lrp5 HBM alleles in Ctsk-Cre expressing cells.

To determine changes in bone mineral content and density among mice with *Ctsk*-Cre-driven activation of *Lrp5* HBM alleles, we collected serial whole body DEXA scans from all experimental mice (Fig 1). *Ctsk*-Cre TG mice with either *Lrp5* HBM allele had increased BMD (5-7% in female, 9-12% in male) and BMC (7-13% in female, 12-15% in male) compared to NTG mice, regardless of sex (Fig 1). There was no difference in BMC and BMD in male TG mice with the +/A or +/G allele, whereas female TG;+/A mice had significantly higher BMC and BMD than TG;+/G mice (Fig 1).

Analysis of the distal femur by µCT indicated that male and female TG;+/A and TG;+/G mice had significantly higher trabecular BV/TV, cortical thickness, and cortical area than their NTG littermates (Fig 2). Vertebral bone mass did not differ between NTG and TG mice for either sex (Fig. S1).

Serum markers of bone resorption and histological measures of osteoclast prevalence are reduced in female but not male mice with Lrp5 mutations induced in Ctsk-Cre-expressing cells

To evaluate osteoclastic activity in these mice, we measured CTx concentration from serum collected at week 7, and we measured the number of, and surface occupied by, osteoclasts in the distal femur metaphysis after sacrifice (Fig 3). Female TG;+/A and TG;+/V mice had reduced serum CTx concentrations (by 10-13%) compared to their NTG littermates, whereas CTx concentrations did not differ in male TG versus NTG mice. Histomorphometric measurements of osteoclast parameters in 16 wk old mice were consistent with the serum CTx concentration results; female TG;+/A and TG;+/G mice had significantly fewer osteoclasts in the distal femur, reaching a 13-16% decrease in OCL surface and a 32-70% reduction in OCL number, compared to their respective NTG littermates. We did not detect any significant differences in osteoclast histological parameters among male mice.

Osteoclast differentiation and activity are reduced in marrow cultures derived from female and not male TG;+/G mice

To determine whether changes in osteoclast-associated measures seen *in vivo* reflect cell autonomous effects of the active Lrp5 allele, we studied osteoclast differentiation and function *in vitro*. Bone marrow-derived hematopoietic stem cells from +/G mice, with or without the *Ctsk*-Cre transgene, were used as a source of OC progenitors, and were induced to differentiate using M-CSF and RANKL. Consistent with what was observed *in vivo*, TRAP staining indicated 45% fewer OCs differentiated *in vitro* from bone marrow progenitors recovered female TG;+/G compared to NTG;+/G mice. Also consistent with the sex specific *in vivo* data, no difference in *in vitro* OC differentiation was observed between male TG;+/G and NTG mice (Fig 4A-4B). The observed sex-related difference in osteoclast formation was not due to initial seeding density, as the same outcome was observed over three different seeding densities (Fig. S1). Additionally, to measure bone resorbing activity of osteoclasts, we re-plated identical numbers of osteoclast-like cells onto bovine cortical bone slices and measured the resorbed ("pit") area after staining. Bone slices containing TG;+/G osteoclasts from female mice had 60% lower pit area than NTG littermate females, while male-derived preparations showed no detectable difference between groups (Fig 4C-4D). Removal of osteoclasts for re-plating onto the bone slices was not associated with a significant loss of, or damage to, cells from female or male mice (Fig. S3). The amount of CTx released into the

culture media was also suppressed in female but not male TG mice (Fig. 4E). Expression of osteoclast-selective genes was reduced in female but not male transgenic mice, compared to respective NTG controls (Fig. 5).

The Ctsk-Cre transgene recombines conditional Lrp5-HBM alleles in bone cells other than osteoclasts, with greater "off-target" recombination occurring in females rather than males.

Although *Ctsk*-Cre is commonly used to induce Cre-mediated recombination in osteoclasts, it may also be active in other skeletal cell types. These "off-target" effects could contribute to the increased bone mass observed in TG;+/A and TG;+/G mice. Because osteocytes express *Ctsk*, particularly under resorption-inducing conditions (26), and since we previously reported that activation of conditional HBM alleles in osteocytes was sufficient to increase bone mass (5), we determined whether the *Ctsk*-Cre transgene was active in cortical bone which is enriched for osteocytes. We extracted DNA from femoral cortical bone of TG;+/G and NTG mice and used ddPCR to measure the percentage of *Lrp5* conditional alleles in this tissue that had recombined. The rate of recombination in NTG mice did not exceed the background level for this assay (<1%). In contrast, male TG;+/G mice had ~8% of their cortical bone *Lrp5* alleles recombined; the rate of cortical bone Lrp5 recombination in female TG;+/G mice was even higher (Fig. 6).

In addition to observing off-target expression in osteocytes, we also noted that the *Ctsk*-Cre TG is active during male gametogenesis. If a sire has the *Ctsk*-Cre TG and a floxed allele, the allele will be inherited recombined in the offspring. This is why all animals in this study inherited the floxed allele from the sire and the *Ctsk*-Cre TG from the dam.

Midshaft femur bone formation parameters are increased on the endocortical but not periosteal surface in mice with Lrp5-HBM mutations induced in Ctsk-Cre-expressing cells

Having found evidence for *Ctsk*-Cre induced Lrp5 HBM activation in osteocytes, we performed dynamic histomorphometry to assess whether some of the increased bone mass in TG;+/A and TG;+/G mice might be due to increased bone formation. Endocortical bone formation (MS/BS and BRF/BS) was significantly increased in male and female TG;+/A mice compared to NTG controls and increased in male, but not female, TG;+/G mice compared to controls (Fig 7). Presence of the TG had no effect on periosteal bone formation.

DISCUSSION

The importance LRP5 signaling to bone anabolism is well known. Mice with global *Lrp5* HBM mutations and mice with conditional activation of the *Lrp5* HBM allele in osteocytes/osteoblasts, had significantly increased bone formation compared to controls (5, 14). Transgenic mice overexpressing a human LRP5 G171V cDNA in osteoblasts ($^{2.3kb}$Col1α1–Lrp5.G171V) also had significantly increased bone formation (15, 27). LRP5 also appears to have a role in preventing bone catabolism. We reported that *Lrp5* HBM mice were protected from the bone catabolic effects of disuse and estrogen deficiency (OVX) (14). Unknown, was whether the HBM mice were protected from catabolism because of anti-osteoclastogenic signals that originated from osteocytes/osteoblasts, from a cell-autonomous role for LRP5 during osteoclast differentiation/function, or both. Experiments in the present communication were designed to address a cell-autonomous role for LRP5 in osteoclasts.

We observed that *Ctsk*-Cre-driven recombination of conditional *Lrp5* HBM alleles led to increased bone mass and architectural properties in male and female mice (Figs 1 and 2), which could be due to increased anabolism or decreased catabolism. In vivo evidence of decreased catabolism was observed in female, but not male, mice (Fig 3). Since osteocytes/osteoblasts help regulate osteoclast activity by expressing RANKL and OPG, we performed *in vitro* osteoclast differentiation and activity assays to determine if the LRP5 effects were cell autonomous. We observed significant reductions in the number of osteoclasts that could be differentiated bone marrow precursors *in vitro* from in female (Fig 4), but not male, TG;+/G mice, and decreased resorptive ability of isolated TG;+/G osteoclasts *ex vivo* (Figs 4 and 5). Taken together, these data are consistent with LRP5 having a cell-autonomous role in osteoclast function; this role appears sex-specific.

Because bone mass was increased in male TG;+/A and TG;+/G mice, despite there being no apparent effect on osteoclast differentiation or resorption, we sought another reason these mice developed increased bone mass. We looked for "off target" recombination of the *Lrp5* HBM allele in osteocytes, for which pro-anabolic roles of LRP5 are known. Osteocytes express Ctsk, albeit at much lower levels than osteoclasts (26). We therefore asked whether *Ctsk*-Cre is also expressed in osteocytes. Droplet digital PCR indicated that Ctsk-Cre was active in ~ 8 to 17% of osteocytes, with females having greater rates of cortical bone recombination than mice. This low, but appreciable, percentage of recombined cells could account for the 2 to 4% increased bone volume fraction and the elevated endocortical bone formation rate seen in TG;+/A and TG;+/G mice (Fig 7). Puzzling, however, is that only endocortical bone formation increased, since global HBM and osteocyte/osteoblast specific activation of HBM alleles increased endocortical and perisosteal bone formation (5). Therefore, we cannot preclude the possibility that increased endocortical bone formation in *Ctsk*-Cre TG mice is the consequence of recombined osteoclasts releasing pro-anabolic coupling factors that affect osteoblasts. The results we obtained using *Ctsk*-Cre to activate Lrp5 HBM alleles are not inconsistent with the results obtained by Weivoda et al (17), who used *Ctsk*-Cre to inactivate Lrp5; they found no effect on bone mass. However, these investigators did show that bone mass was reduced when Lrp5 was inactivated using a different and earlier-acting osteoclast Cre driver (Rank-Cre) (17).

In conclusion, our results support the hypothesis that there is a cell-autonomous role for LRP5 in osteoclasts. In female mice, *Ctsk*-Cre mediated activation of Lrp5 HBM alleles reduced osteoclast differentiation and bone resorbing activity *in vivo* and *in vitro*. Ctsk-Cre mediated activation of Lrp5 HBM alleles also significantly increased bone mass in male mice, however the mechanism is less certain. It is possible that osteoclasts with active Lrps5 HBM alleles released pro-anabolic factors that affected osteoblasts. Alternatively, "off target" Ctsk-Cre activity in a small percentage of osteocytes may have been sufficient to promote increased endocortical bone formation. Additional experiments are needed to address these two possibilities.

FIGURE LEGENDS

Fig 1. Increased bone DEXA values in mice with activated *Lrp5* HBM alleles in *Ctsk*-Cre expressing cells. (A) Schematic diagram of the experimental design. (B - E) Skeletal mass and density were increased significantly in *Lrp5* HBM conditional mice (+/A or +/G) when the Ctsk-Cre transgene was present (TG, open symbols) compared to non-transgenic mice (NTG, filled symbols). Whole body bone mineral content (WB BMC) and density (WB BMC) were measured by DXA at 7, 10, and 15 weeks using an ROI that encompassed the entire postcranial skeleton of (B and C) female and (D and E) male mice. * $p < 0.05$ compared to Lrp5-matched NTG counterpart, † $p < 0.05$ compared to +/G TG mice. Sample size is n=11/group.

Fig 2. Increased bone μCT values in mice with activated *Lrp5* HBM alleles in *Ctsk*-Cre expressing cells. (A) Trabecular bone volume fraction (Tb.BV/TV), (B) cortical thickness (Ct.Th), and (C) cortical area (Ct.Ar) were measured in the femora of 16-week-old female Lrp5 heterozygous +/A and +/G mice, with (+) or without (-) the Ctsk-Cre transgene (* $p < 0.05$ compared to each NTG counterpart, + $p < 0.05$ compared to +/A TG mice). (D) Representative μCT reconstructions of the distal femur of all female experimental groups. (E-G) Same parameters measured in femora from 16-week-old male mice. (* $p < 0.05$ compared to each NTG counterpart, † $p < 0.05$ compared to +/G TG mice). (F) Representative μCT reconstructions of the distal femur of all male experimental groups. Sample size in n=11/group.

Fig 3. Reduced bone resorption in female, but not male, mice with activated *Lrp5* HBM alleles in *Ctsk*-Cre expressing cells. The resorption marker carboxyl-terminal collagen crosslinks (CTx) was measured from serum collected from (A) female and (D) male Lrp5 heterozygous +/A and +/G mice, with (+) or without (-) the Ctsk-Cre transgene at 7 weeks of age. Osteoclast surface per bone surface (Oc.S/BS; panels B and E) and number of osteoclast per bone surface (N.Oc/BS; panels C and F) were measured in the distal femoral metaphysis in sections from 16-week-old mice by counting tartrate-resistant acid phosphatase (TRAP)-positive cells over bone surface. * $p < 0.05$ compared to each Cre-negative counterpart, † $p < 0.05$ compared to +/G Cre-positive mice. Sample size in n=11/group.

Fig 4. Reduced *in vitro* osteoclastic differentiation and bone resorption in female, but not male, mice with activated *Lrp5* HBM alleles in *Ctsk*-Cre expressing cells. Photomicrographs (A) and graph (B) depicting TRAP stained OCs differentiated from bone marrow, Photomicrograph (C) and graph (D) depicting TRAP stained resorption pit assays, and (E) graph depicting. ELISA-based quantitation of C-terminal telopeptide (CTx) released into the media after 3 days of culture, standardized by osteoclast number (Oc.N). * $p < 0.05$ compared to NTG counterpart. Sample size in n=3/group.

Fig. 5. *In vitro* assessment of transcripts associated with osteoclastogenesis and maturity in macrophages (MQ; day 0 of culture from BMMs), preosteoclasts (day 2 of culture in osteoclast-differentiating conditions), and mature osteoclasts (day 4 in osteoclast-differentiating conditions). Quantitative PCR was used to measure expression of (A) osteoclast associated, immunoglobulin-like receptor (*Oscar*), (B) Dendrocyte expressed seven transmembrane protein (*Dcstamp*), (C) Cathepsin-K (*Ctsk*), (D) Chloride voltage-gated channel 7 (*Clcn7*), and (E) V-type proton ATPase (*Atp6ap1*). Expression levels for each gene were normalized to *Gapdh* expression. * $p < 0.05$ compared to NTG counterpart. Sample size in n=3/group.

Fig 6. *Ctsk*-Cre is active in bone cells other than osteoclasts. (A) Schematic depicting a portion of the Lrp5 HBM conditional alleles. The ddPCR assay was designed distinguish non-recombined (neo-containing) and recombined (neo-excised) alleles. (B) Scatterplots depicting ddPCR results using cortical bone DNA from $Lrp5^{+/+}$ mice (B_1, which contain only empty droplets in the bottom left quadrant), $Lrp5^{+/G_N}$ mice without the Ctsk-Cre TG (B_2, which also contains droplets with non-recombined alleles ["cond"] in the right lower quadrant), and $Lrp5^{+/G_N}$ mice with the *Ctsk*-Cre TG (B_3, which now also contains recombined alleles ["rec"] in the left upper quadrant. Graph depicting mean percentages of recombined alleles (± 1SD) in male +/G, male TG;+/G, and female TG;+/G mice. * $p < 0.05$ compared to NTG samples, † $p< 0.05$ compared to the TG;+/G male samples. Sample size is n=3/group, and each DNA sample was assayed in triplicate.

Fig 7. Increased endocortical, but not perisosteal, bone formation in mice with activated *Lrp5* HBM alleles in *Ctsk*-Cre expressing cells. Bone formation parameters were measured in the femoral midshaft from 16-week-old (A-F) female and (G-L) male mice by mineralizing surface per bone surface (MS/BS), mineral apposition rate (MAR), and bone formation rate per unit bone surface (BFR/BS). Endocortical (A-C, G-I) and periosteal (D-F, J-L) were analyzed separately. Both female and male TG mice gained new bones on endocortical region compared to each counterpart but the bone gain in TG;+/G female mice was not significant compared to NTG;+/G female mice. Periosteal BFR/BS in females and males was not statistically noticeable. * $p < 0.05$ compared to each NTG counterpart. Sample size in n=11/group.

SUPPLEMENTARY FIGURE LEGENDS

Fig. S1. Lrp5-HBM mutations induced in Ctsk-expressing cells resulted in similar vertebral (5^{th} lumbar vertebra) trabecular bone mass compared to those without the Ctsk-Cre transgene, in both (A) female and (B) male mice.

Fig. S2. Osteoclast formation is impaired in female but not male transgenic mice, regardless of initial seeding density. Three different initial seeding densities of osteoclasts were assayed for Trap staining (3×10^4, 6×10^4, and 9×10^4 per well of a 96-well plate) after 4-5 days of culture. Regardless of the initial seeding density, the size and the number of osteoclasts from female TG mice were significantly lower than all other groups, although the overall number of mature osteoclasts (>3 nuclei) was greater with higher number of initial cells.

Fig. S3. Osteoclasts were differentiated in 48 well culture dishes as described in the methods. Mature multinucleated cells were enumerated before being detached with trypsin, and then reseeded into culture wells and counted again after 6 hr. Approximately 85-90% of the original osteoclast number was recovered after reseeding, regardless of the sex or genotype of the starting culture. The number of osteoclasts from female TG mice were significantly lower than the other groups before and after reseeding, indicating that reseeding had no effect on the observed female-specific decrease in osteoclast number.

REFERENCES

1. Canalis E. Wnt signalling in osteoporosis: mechanisms and novel therapeutic approaches. *Nat Rev Endocrinol.* 2013;9(10):575-83.
2. Cairoli E, Zhukouskaya VV, Eller-Vainicher C, and Chiodini I. Perspectives on osteoporosis therapies. *Journal of endocrinological investigation.* 2015;38(3):303-11.
3. Lerner UH, and Ohlsson C. The WNT system: background and its role in bone. *Journal of internal medicine.* 2015;277(6):630-49.
4. Kang KS, and Robling AG. New Insights into Wnt-Lrp5/6-beta-Catenin Signaling in Mechanotransduction. *Frontiers in endocrinology.* 2014;5(246.
5. Cui Y, Niziolek PJ, MacDonald BT, Zylstra CR, Alenina N, Robinson DR, Zhong Z, Matthes S, Jacobsen CM, Conlon RA, et al. Lrp5 functions in bone to regulate bone mass. *Nat Med.* 2011;17(6):684-91.
6. Little RD, Carulli JP, Del Mastro RG, Dupuis J, Osborne M, Folz C, Manning SP, Swain PM, Zhao SC, Eustace B, et al. A mutation in the LDL receptor-related protein 5 gene results in the autosomal dominant high-bone-mass trait. *Am J Hum Genet.* 2002;70(1):11-9.
7. Balemans W, Ebeling M, Patel N, Van Hul E, Olson P, Dioszegi M, Lacza C, Wuyts W, Van Den Ende J, Willems P, et al. Increased bone density in sclerosteosis is due to the deficiency of a novel secreted protein (SOST). *Human molecular genetics.* 2001;10(5):537-43.
8. Gong Y, Slee RB, Fukai N, Rawadi G, Roman-Roman S, Reginato AM, Wang H, Cundy T, Glorieux FH, Lev D, et al. LDL receptor-related protein 5 (LRP5) affects bone accrual and eye development. *Cell.* 2001;107(4):513-23.
9. Sawakami K, Robling AG, Ai M, Pitner ND, Liu D, Warden SJ, Li J, Maye P, Rowe DW, Duncan RL, et al. The Wnt co-receptor LRP5 is essential for skeletal mechanotransduction but not for the anabolic bone response to parathyroid hormone treatment. *The Journal of biological chemistry.* 2006;281(33):23698-711.
10. Ai M, Holmen SL, Van Hul W, Williams BO, and Warman ML. Reduced affinity to and inhibition by DKK1 form a common mechanism by which high bone mass-associated missense mutations in LRP5 affect canonical Wnt signaling. *Mol Cell Biol.* 2005;25(12):4946-55.
11. Bhat BM, Allen KM, Liu W, Graham J, Morales A, Anisowicz A, Lam HS, McCauley C, Coleburn V, Cain M, et al. Structure-based mutation analysis shows the importance of LRP5 beta-propeller 1 in modulating Dkk1-mediated inhibition of Wnt signaling. *Gene.* 2007;391(1-2):103-12.
12. Boyden LM, Mao J, Belsky J, Mitzner L, Farhi A, Mitnick MA, Wu D, Insogna K, and Lifton RP. High bone density due to a mutation in LDL-receptor-related protein 5. *The New England journal of medicine.* 2002;346(20):1513-21.
13. Semenov MV, and He X. LRP5 mutations linked to high bone mass diseases cause reduced LRP5 binding and inhibition by SOST. *The Journal of biological chemistry.* 2006;281(50):38276-84.
14. Niziolek PJ, Bullock W, Warman ML, and Robling AG. Missense Mutations in LRP5 Associated with High Bone Mass Protect the Mouse Skeleton from Disuse- and Ovariectomy-Induced Osteopenia. *PLoS One.* 2015;10(11):e0140775.
15. Saxon LK, Jackson BF, Sugiyama T, Lanyon LE, and Price JS. Analysis of multiple bone responses to graded strains above functional levels, and to disuse, in mice in vivo show that the human Lrp5 G171V High Bone Mass mutation increases the osteogenic response to loading but that lack of Lrp5 activity reduces it. *Bone.* 2011;49(2):184-93.
16. Teitelbaum SL, and Ross FP. Genetic regulation of osteoclast development and function. *Nature reviews Genetics.* 2003;4(8):638-49.
17. Weivoda MM, Ruan M, Hachfeld CM, Pederson L, Howe A, Davey RA, Zajac JD, Kobayashi Y, Williams BO, Westendorf JJ, et al. Wnt Signaling Inhibits Osteoclast Differentiation by Activating Canonical and Noncanonical cAMP/PKA Pathways. *J Bone Miner Res.* 2016;31(1):65-75.
18. Yang T, Zhang J, Cao Y, Zhang M, Jing L, Jiao K, Yu S, Chang W, Chen D, and Wang M. Wnt5a/Ror2 mediates temporomandibular joint subchondral bone remodeling. *Journal of dental research.* 2015;94(6):803-12.
19. Haxaire C, Hay E, and Geoffroy V. Runx2 Controls Bone Resorption through the Down-regulation of the Wnt Pathway in Osteoblasts. *The American journal of pathology.* 2016.

20. Chiu WS, McManus JF, Notini AJ, Cassady AI, Zajac JD, and Davey RA. Transgenic mice that express Cre recombinase in osteoclasts. *Genesis.* 2004;39(3):178-85.
21. Robling AG, Kedlaya R, Ellis SN, Childress PJ, Bidwell JP, Bellido T, and Turner CH. Anabolic and catabolic regimens of human parathyroid hormone 1-34 elicit bone- and envelope-specific attenuation of skeletal effects in Sost-deficient mice. *Endocrinology.* 2011;152(8):2963-75.
22. Kedlaya R, Kang KS, Hong JM, Bettagere V, Lim KE, Horan D, Divieti-Pajevic P, and Robling AG. Adult-Onset Deletion of beta-Catenin in (10kb)Dmp1-Expressing Cells Prevents Intermittent PTH-Induced Bone Gain. *Endocrinology.* 2016;157(8):3047-57.
23. Hong JM, Teitelbaum SL, Kim TH, Ross FP, Kim SY, and Kim HJ. Calpain-6, a target molecule of glucocorticoids, regulates osteoclastic bone resorption via cytoskeletal organization and microtubule acetylation. *Journal of bone and mineral research : the official journal of the American Society for Bone and Mineral Research.* 2011;26(3):657-65.
24. Luks VL, Kamitaki N, Vivero MP, Uller W, Rab R, Bovee JV, Rialon KL, Guevara CJ, Alomari AI, Greene AK, et al. Lymphatic and other vascular malformative/overgrowth disorders are caused by somatic mutations in PIK3CA. *J Pediatr.* 2015;166(4):1048-54 e1-5.
25. Dempster DW, Compston JE, Drezner MK, Glorieux FH, Kanis JA, Malluche H, Meunier PJ, Ott SM, Recker RR, and Parfitt AM. Standardized nomenclature, symbols, and units for bone histomorphometry: a 2012 update of the report of the ASBMR Histomorphometry Nomenclature Committee. *J Bone Miner Res.* 2013;28(1):2-17.
26. Qing H, Ardeshirpour L, Pajevic PD, Dusevich V, Jahn K, Kato S, Wysolmerski J, and Bonewald LF. Demonstration of osteocytic perilacunar/canalicular remodeling in mice during lactation. *J Bone Miner Res.* 2012;27(5):1018-29.
27. Babij P, Zhao W, Small C, Kharode Y, Yaworsky PJ, Bouxsein ML, Reddy PS, Bodine PV, Robinson JA, Bhat B, et al. High bone mass in mice expressing a mutant LRP5 gene. *Journal of bone and mineral research : the official journal of the American Society for Bone and Mineral Research.* 2003;18(6):960-74.

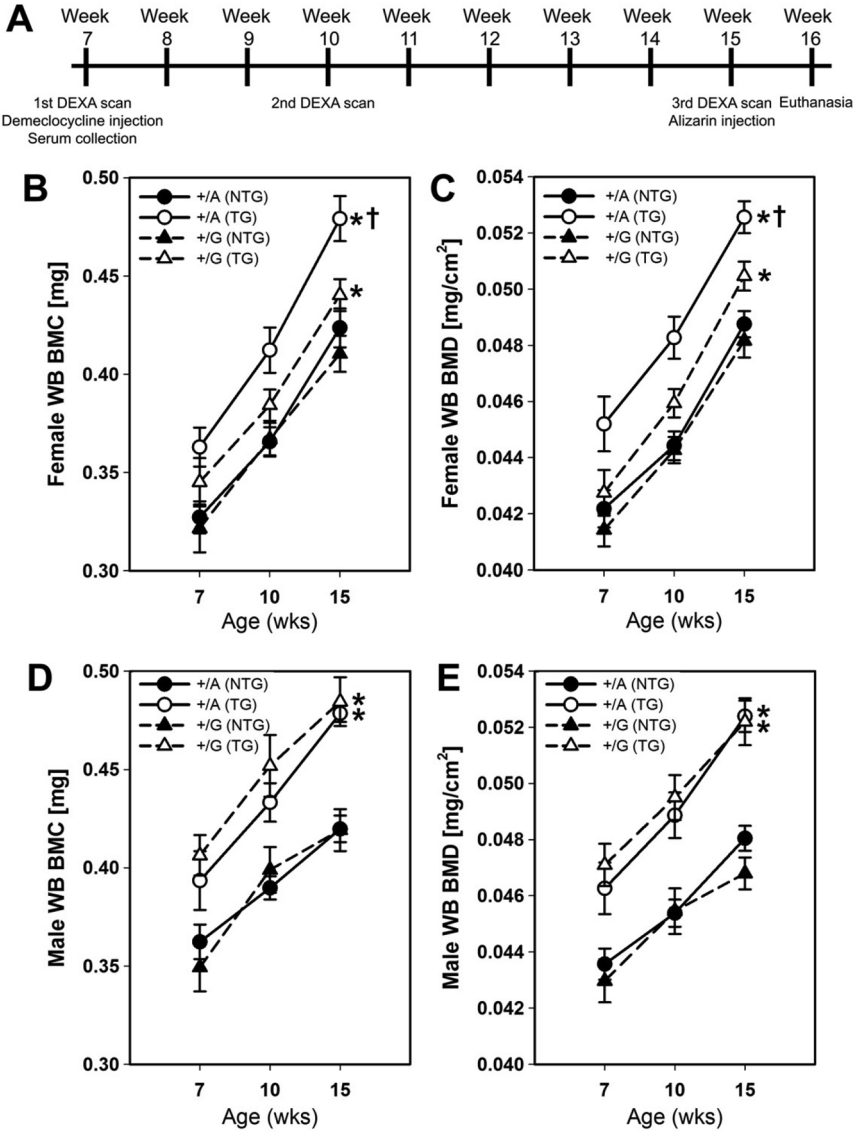
A
Week 7
Week 8
Week 9
Week 10
Week 11
Week 12
Week 13
Week 14
Week 15
Week 16
1st DEXA scan
Demeclocycline injection
Serum collection
2nd DEXA scan
3rd DEXA scan
Alizarin injection
Euthanasia
B
Female WB BMC [mg]
C
Female WB BMD [mg/cm2]
D
Male WB BMC [mg]
E
Male WB BMD [mg/cm2]
+/A (NTG)
+/A (TG)
+/G (NTG)
+/G (TG)
Age (wks)

Figure 1

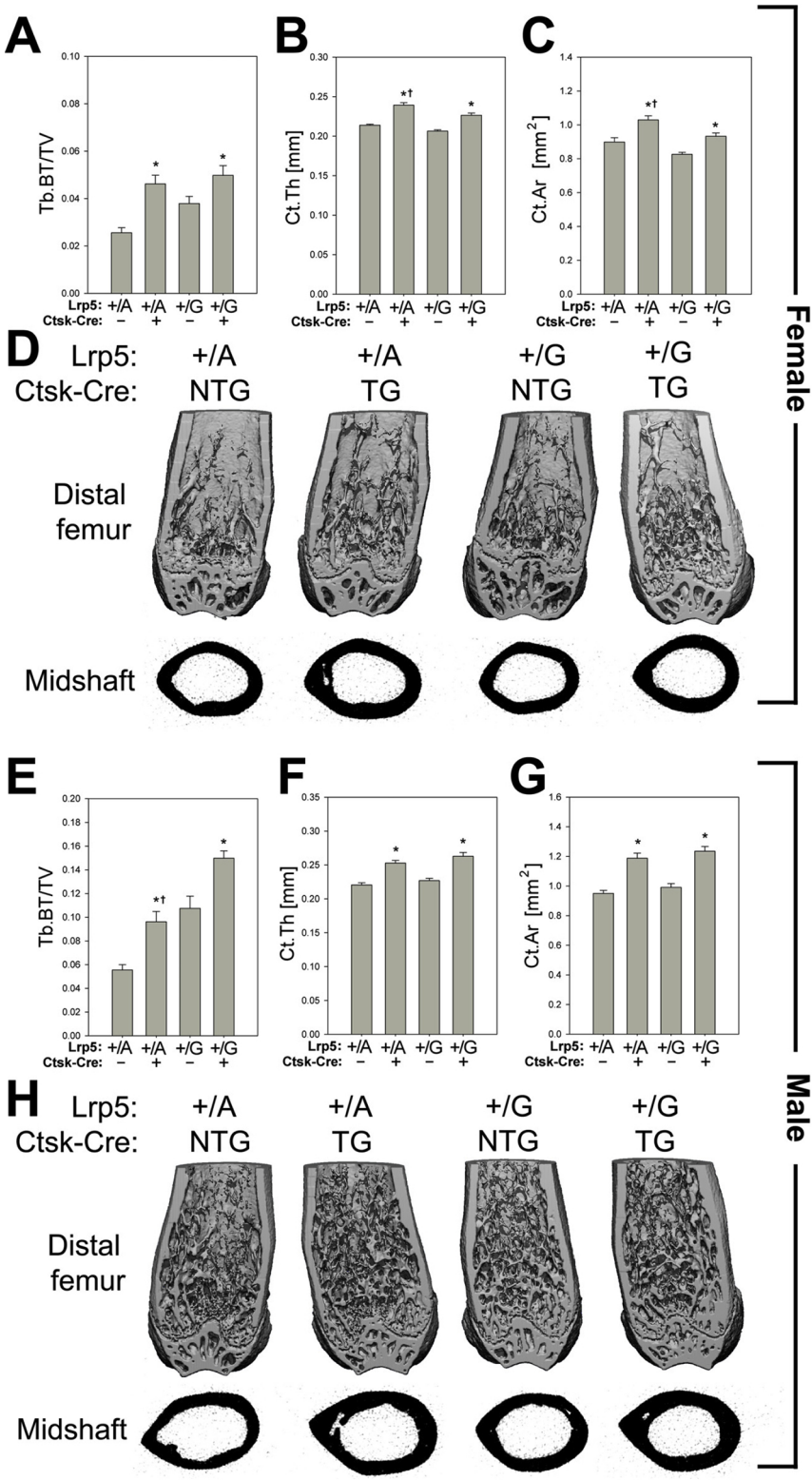
A
Tb.BT/TV
B
Ct.Th [mm]
C
Ct.Ar [mm²]
Lrp5: +/A +/A +/G +/G
Ctsk-Cre: – + – +
Female
D
Lrp5: +/A +/A +/G +/G
Ctsk-Cre: NTG TG NTG TG
Distal femur
Midshaft
E
Tb.BT/TV
F
Ct.Th [mm]
G
Ct.Ar [mm²]
Male
H
Lrp5: +/A +/A +/G +/G
Ctsk-Cre: NTG TG NTG TG
Distal femur
Midshaft

Figure 2

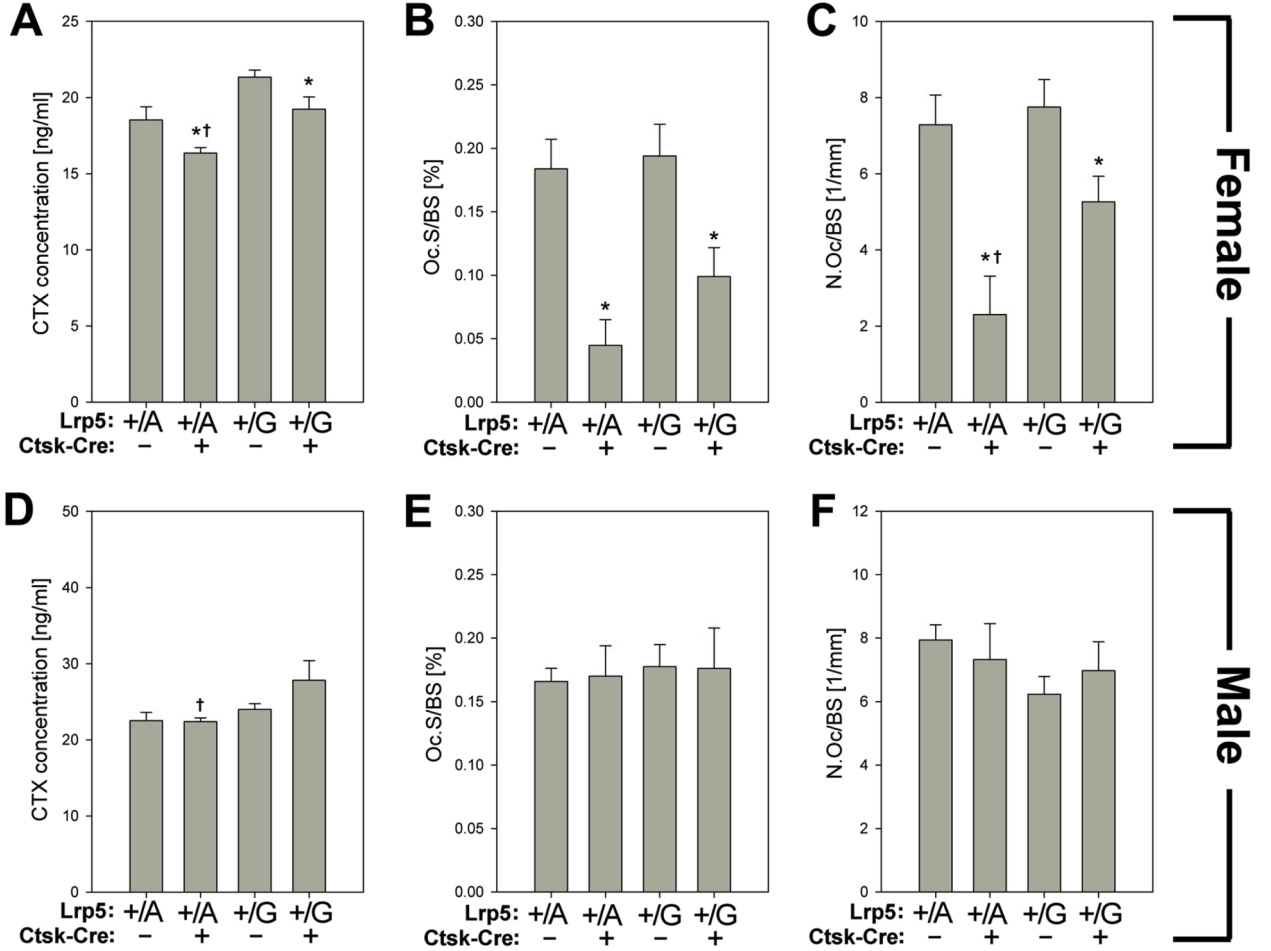
A
CTX concentration [ng/ml]
25
20
15
10
5
0
*†
*
B
Oc.S/BS [%]
0.30
0.25
0.20
0.15
0.10
0.05
0.00
*
*
C
N.Oc/BS [1/mm]
10
8
6
4
2
0
*†
*
Lrp5: +/A +/A +/G +/G
Ctsk-Cre: – + – +
Female
D
CTX concentration [ng/ml]
50
40
30
20
10
0
†
E
Oc.S/BS [%]
0.30
0.25
0.20
0.15
0.10
0.05
0.00
F
N.Oc/BS [1/mm]
12
10
8
6
4
2
0
Lrp5: +/A +/A +/G +/G
Ctsk-Cre: – + – +
Male

Figure 3

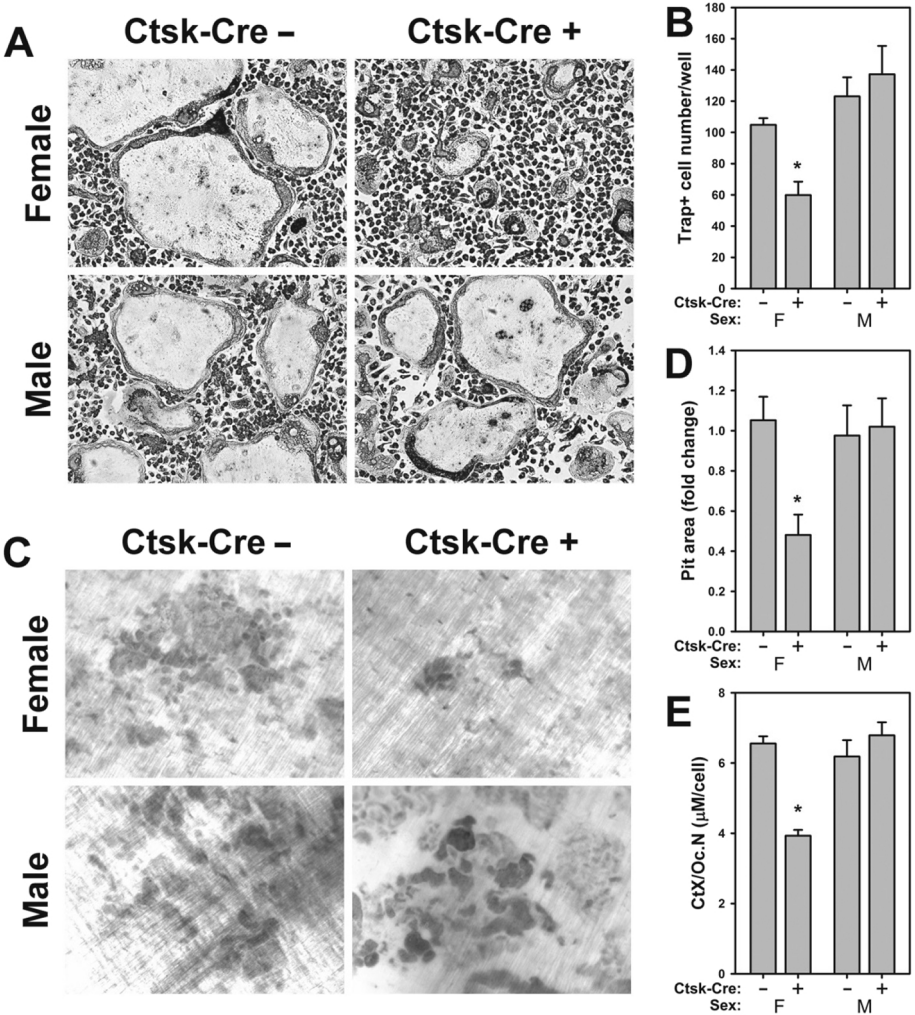
A
Ctsk-Cre –
Ctsk-Cre +
Female
Male
B
Trap+ cell number/well
0
20
40
60
80
100
120
140
160
180
*
Ctsk-Cre: – + – +
Sex: F M
C
Ctsk-Cre –
Ctsk-Cre +
Female
Male
D
Pit area (fold change)
0.0
0.2
0.4
0.6
0.8
1.0
1.2
1.4
*
Ctsk-Cre: – + – +
Sex: F M
E
CtX/Oc.N (μM/cell)
0
2
4
6
8
*
Ctsk-Cre: – + – +
Sex: F M

Figure 4

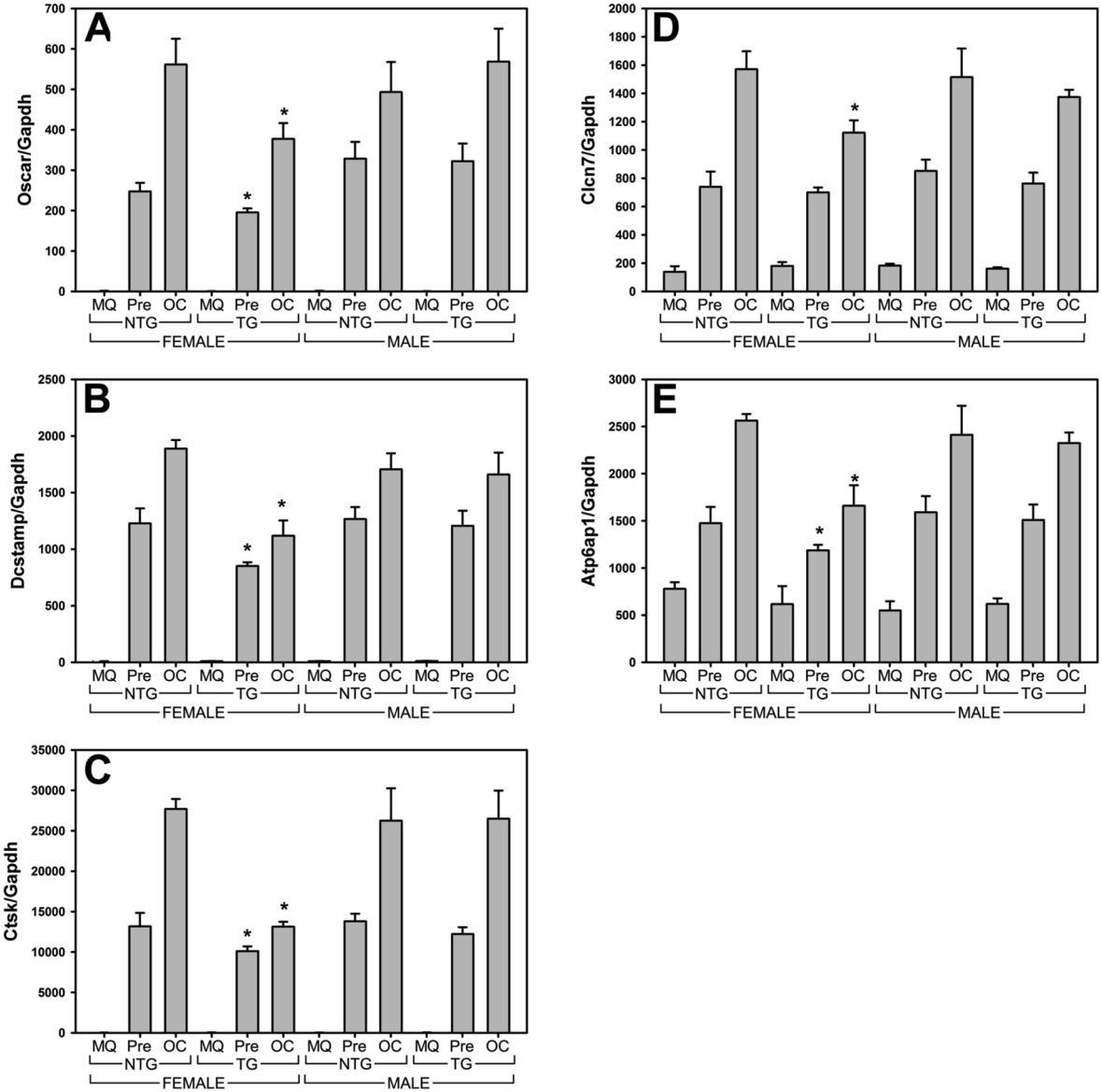
A
Oscar/Gapdh
700
600
500
400
300
200
100
0
B
Dcstamp/Gapdh
2500
2000
1500
1000
500
0
C
Ctsk/Gapdh
35000
30000
25000
20000
15000
10000
5000
0
D
Clcn7/Gapdh
2000
1800
1600
1400
1200
1000
800
600
400
200
0
E
Atp6ap1/Gapdh
3000
2500
2000
1500
1000
500
0
MQ Pre OC MQ Pre OC MQ Pre OC MQ Pre OC
NTG TG NTG TG
FEMALE MALE
*

Figure 5

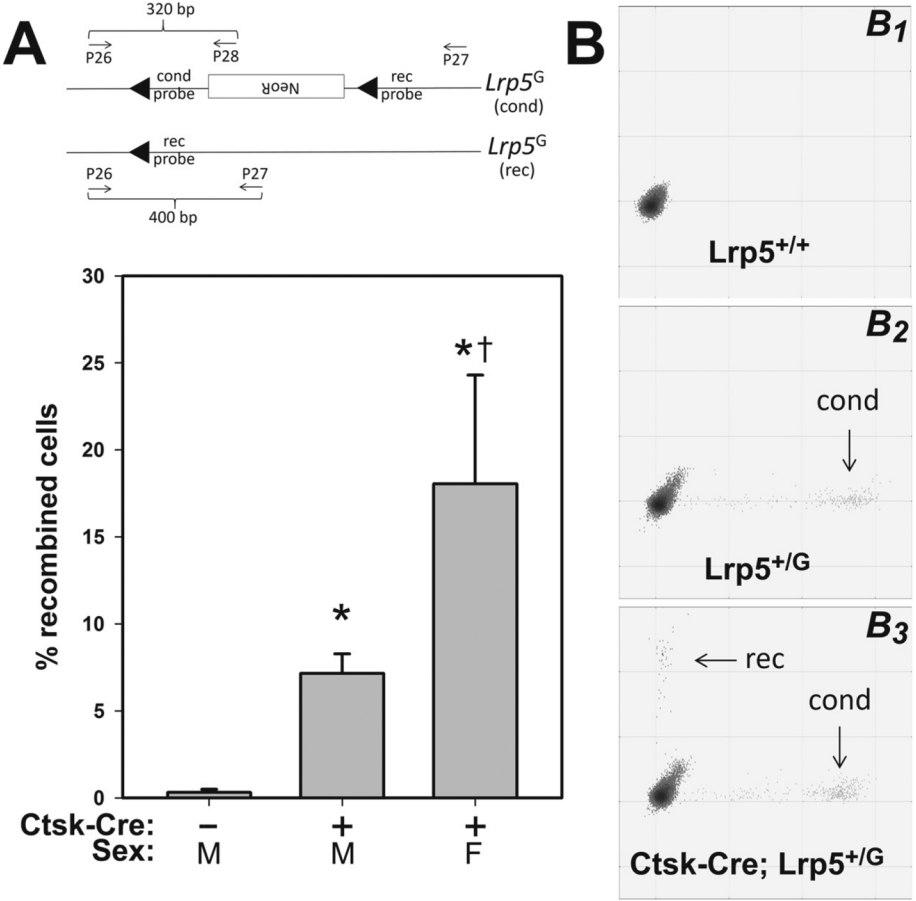
A
320 bp
P26
P28
P27
cond probe
NeoR
rec probe
Lrp5G (cond)
rec probe
Lrp5G (rec)
P26
P27
400 bp
B
B1
Lrp5+/+
B2
cond
Lrp5+/G
B3
rec
cond
Ctsk-Cre; Lrp5+/G
% recombined cells
30
25
20
15
10
5
0
*
*†
Ctsk-Cre:
Sex:
–
+
+
M
M
F

Figure 6

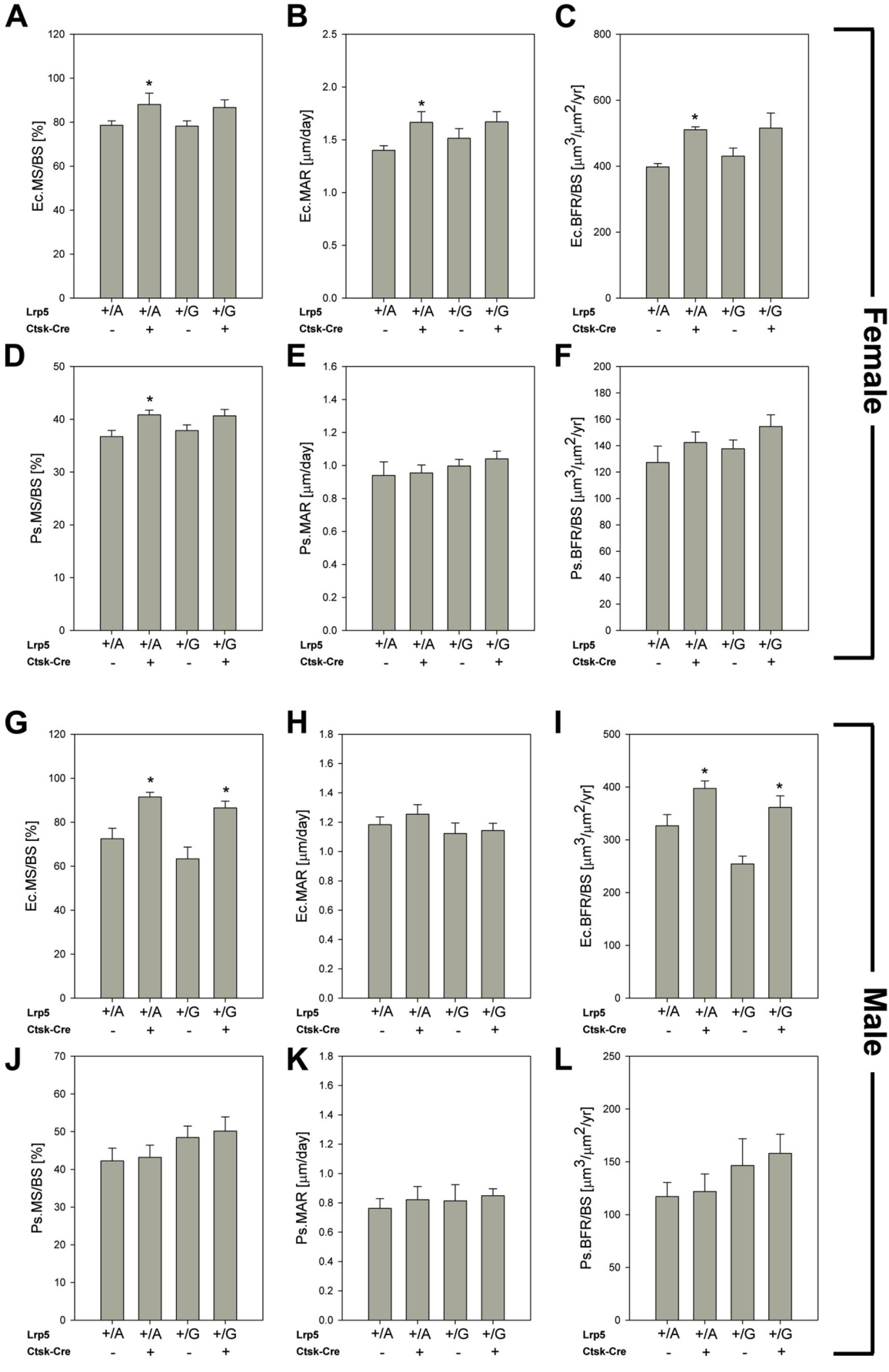
A
B
C
D
E
F
G
H
I
J
K
L
Female
Male
Ec.MS/BS [%]
Ec.MAR [μm/day]
Ec.BFR/BS [μm3/μm2/yr]
Ps.MS/BS [%]
Ps.MAR [μm/day]
Ps.BFR/BS [μm3/μm2/yr]
Lrp5 +/A +/A +/G +/G
Ctsk-Cre - + - +

Figure 7